Continuum kinetic model for simulating low-collisionality regimes in plasmas

G. V. Vogman
Applied Science and Technology Program
University of California — Berkeley
Berkeley, CA 94704
Email: geniav@berkeley.edu

P. Colella
Applied Numerical Algorithms Group
Lawrence Berkeley National Laboratory
1 Cyclotron Road Berkeley, CA 94720
Email: pcolella@lbl.gov

***Abstract*—Continuum kinetic models, such as Maxwell-Boltzmann, present a viable alternative to particle-in-cell (PIC) models because they can be cast in conservation form and are not susceptible to noise. By treating the associated phase space distribution function as a continuous incompressible fluid occupying a volume of position-velocity space, evolution of the distribution function is determined by solving a 6-D advection equation. In cases where collision terms are negligible, the Boltzmann model is reduced to a Vlasov model. A 4th-order accurate continuum kinetic Vlasov model has been developed in one spatial and one velocity dimension to address the challenges associated with solving a hyperbolic governing equation in multidimensional phase space. The governing equation is cast in conservation law form and solved with a finite volume representation. Adaptive mesh refinement (AMR) is used to allow for efficient use of computational resources while maintaining desired levels of resolution. Consequently, with AMR the model is able to capture the fine structures that develop in the distribution function as it evolves in time, while using low resolution in the tail of the distribution function. The model is tested on several plasma phenomena including: weak and strong Landau damping and the two-stream instability. Conservation properties of the method are investigated.**

I. Introduction

In statistical plasma kinetic theory, each particle species is treated as a distribution function evolving in position-velocity phase space. For a collisionless plasma, the evolution is described by a coupled system of partial differential equations: the Vlasov equation and Maxwell's equations. When solved in its most general form, this model has six dimensions — three spatial coordinates and three velocity coordinates — thereby making it computationally costly. For this reason, particle-in-cell (PIC) methods, which rely on sampling the distribution function, have been the dominant means of solving this system. Due to recent advancements in supercomputing technology, however, full phase-space continuum methods have garnered more attention and have become a viable means of simulating nonlinear plasma kinetics. [2], [3], [4], [1], [7]

Continuum methods are advantageous because they can be cast in conservation-law form and thereby be solved using flux-based techniques that have been well-developed in the field of hyperbolic partial differential equations. Hyperbolic solvers also allow for: straightforward parallelization based on domain decomposition; the use of adaptive mesh refinement (AMR) techniques; and numerical methods that are high-order accurate in space and time.[2] Parallel AMR can, in particular, be used to reduce the cost of a continuum multi-dimensional Vlasov simulation by focusing computational resources in dynamic parts of the domain. Moreover, continuum methods do not suffer from sampling-associated noise seen in PIC methods [9] and can thus produce more physically accurate results.

The content of this paper investigates a high-order accurate numerical method for modeling the electrostatic regime represented by the Vlasov-Poisson system in one spatial and one velocity dimension. The unsplit finite volume method is fourth-order accurate in time and space and solves the system of equations in conservation-law form. The method is benchmarked against analytic results for weak Landau damping, strong Landau damping, and two-stream instability evolution. Its conservation properties are assessed and results with adaptive mesh refinement are presented.

II. Vlasov-Poisson System and Underlying Assumptions

Plasma evolution timescales over which electrons are dynamic and ions remain static are considered. In such a system there is only one evolving distribution function $f(x, v, t)$ — that of the electrons. Assuming collisions have negligible effect means the plasma kinetics can be modeled by the Vlasov equation [8] in conservation-law form:

$$0 = \frac{\partial f}{\partial t} + \frac{\partial}{\partial x}(vf) - \frac{e}{m}\frac{\partial}{\partial v}(Ef), \tag{1}$$

where f is the distribution function, t is time, x is the phase space position coordinate, v is the phase space x-direction velocity coordinate, e is the absolute value of electron charge, m is the electron mass, and E is the electric field in the x-direction. In Eq. 1 only electrostatic forces are considered such that currents and magnetic fields are assumed to be negligible. The electric potential, ϕ, is calculated using Poisson's equation in one dimension,

$$\frac{\partial^2 \phi}{\partial x^2} = -\frac{\rho_c}{\varepsilon_0}, \tag{2}$$

where ρ_c is the charge density and ε_0 is the vacuum permittivity. Note that the electric field is related to the gradient of

978-1-4673-5168-3/13/$31.00 ©2013 IEEE

Report Documentation Page

Form Approved
OMB No. 0704-0188

1. REPORT DATE	2. REPORT TYPE	3. DATES COVERED
JUN 2013	**N/A**	**-**

4. TITLE AND SUBTITLE
Continuum kinetic model for simulating low-collisionality regimes in plasmas

5a. CONTRACT NUMBER
5b. GRANT NUMBER
5c. PROGRAM ELEMENT NUMBER

6. AUTHOR(S)

5d. PROJECT NUMBER
5e. TASK NUMBER
5f. WORK UNIT NUMBER

7. PERFORMING ORGANIZATION NAME(S) AND ADDRESS(ES)
Applied Science and Technology Program University of California Berkeley Berkeley, CA 94704

8. PERFORMING ORGANIZATION REPORT NUMBER

9. SPONSORING/MONITORING AGENCY NAME(S) AND ADDRESS(ES)

10. SPONSOR/MONITOR'S ACRONYM(S)
11. SPONSOR/MONITOR'S REPORT NUMBER(S)

12. DISTRIBUTION/AVAILABILITY STATEMENT
Approved for public release, distribution unlimited

13. SUPPLEMENTARY NOTES
See also ADM002371. 2013 IEEE Pulsed Power Conference, Digest of Technical Papers 1976-2013, and Abstracts of the 2013 IEEE International Conference on Plasma Science. IEEE International Pulsed Power Conference (19th). Held in San Francisco, CA on 16-21 June 2013, The original document contains color images.

14. ABSTRACT
Continuum kinetic models, such as Maxwell- Boltzmann, present a viable alternative to particle-in-cell (PIC) models because they can be cast in conservation form and are not susceptible to noise. By treating the associated phase space distribution function as a continuous incompressible fluid occupying a volume of position-velocity space, evolution of the distribution function is determined by solving a 6-D advection equation. In cases where collision terms are negligible, the Boltzmann model is reduced to a Vlasov model. A 4th-order accurate continuum kinetic Vlasov model has been developed in one spatial and one velocity dimension to address the challenges associated with solving a hyperbolic governing equation in multidimensional phase space. The governing equation is cast in conservation law form and solved with a finite volume representation. Adaptive mesh refinement (AMR) is used to allow for efficient use of computational resources while maintaining desired levels of resolution. Consequently, with AMR the model is able to capture the fine structures that develop in the distribution function as it evolves in time, while using low resolution in the tail of the distribution function. The model is tested on several plasma phenomena including: weak and strong Landau damping and the two-stream instability. Conservation properties of the method are investigated.

15. SUBJECT TERMS

16. SECURITY CLASSIFICATION OF:			17. LIMITATION OF ABSTRACT	18. NUMBER OF PAGES	19a. NAME OF RESPONSIBLE PERSON
a. REPORT **unclassified**	b. ABSTRACT **unclassified**	c. THIS PAGE **unclassified**	**SAR**	**5**	

Standard Form 298 (Rev. 8-98)
Prescribed by ANSI Std Z39-18

the potential: $E = -\nabla\phi$. The charge density is defined as

$$\rho_c(x) = e\left[1 - \int_{-\infty}^{\infty} f(x,v,t)dv\right] \tag{3}$$

Because the system is assumed to be non-relativistic, the range over which velocity is defined is unbounded, meaning in theory that $v \in (-\infty, \infty)$. In practice, i.e. in numerical simulations, the velocity is bounded by some sufficiently high value v_{max} such that $v \in [-v_{max}, v_{max}]$. The value of v_{max} is set such that $f(x, \pm v_{max})|_{t=0}$ is zero to machine precision. The distribution function $f(x,v,t)$ is normalized such that the net charge density over the entire spatial domain is zero.

The kinetic energy and potential energy for the Vlasov-Poisson system are defined as follows [5]

$$KE = \frac{1}{2} m \int\int v^2 f dv dx \tag{4}$$

$$PE = \frac{1}{2}\varepsilon_0 \int E^2 dx. \tag{5}$$

The values of kinetic and potential energy provide a useful means of comparing results of numerical simulations to theoretical predictions. The values of energy also provide a metric by which to evaluate conservation properties of the Vlasov-Poisson solver.

III. Discretization and Integration in Time

A fourth-order finite volume method is employed to advance the solution $f(x,v)$ in time. This is done by first initializing the distribution function by a fourth-order cell-average of the analytic initial condition, f_0, at discrete set of points i, j, denoting the spatial and velocity index, respectively. Thus at time $t = 0$ the cell-average distribution function to fourth order is

$$\langle f\rangle_{i,j} = f_0(ih_x, jh_v) + \frac{h_x^2}{24}\frac{\partial^2 f_0}{\partial x^2} + \frac{h_v^2}{24}\frac{\partial^2 f_0}{\partial v^2}. \tag{6}$$

Note that $\langle\cdot\rangle$ denotes the average value over a cell

$$\langle f\rangle_{i,j} = \frac{1}{h_x h_v}\int_{(i-\frac{1}{2})h_x}^{(i+\frac{1}{2})h_x}\int_{(j-\frac{1}{2})h_v}^{(j+\frac{1}{2})h_v} f(x,v)dvdx \tag{7}$$

and h_x and h_v refer to cell widths in the x and v directions. The second derivative terms on the right hand side of Eq. 6 are defined using a second-order accurate centered difference stencil

$$\frac{\partial^2 f_0}{\partial v^2} = \frac{f_{i,j+1} - 2f_{i,j} + f_{i,j-1}}{h_v^2} \tag{8}$$

$$\frac{\partial^2 f_0}{\partial x^2} = \frac{f_{i+1,j} - 2f_{i,j} + f_{i-1,j}}{h_x^2}. \tag{9}$$

The value of the cell-average potential $\langle\phi\rangle_i$ is computed from a fourth-order finite volume stencil for the Poisson equation [10]

$$\begin{aligned} -\frac{1}{\varepsilon_0}\langle\rho_c\rangle_i h_x^2 = &-\frac{1}{12}\langle\phi\rangle_{i+2} + \frac{4}{3}\langle\phi\rangle_{i+1} - \frac{5}{2}\langle\phi\rangle_i \\ &+ \frac{4}{3}\langle\phi\rangle_{i-1} - \frac{1}{12}\langle\phi\rangle_{i-2}, \end{aligned} \tag{10}$$

where $\langle\rho_c\rangle_i$ is defined in terms of the zeroth moment of the cell-average distribution,

$$\langle\rho_c\rangle_i = 1 - h_v\sum_j \langle f\rangle_{i,j}. \tag{11}$$

The cell-average electric field is computed from the potential:

$$\begin{aligned} \langle E\rangle_i = &-\frac{8}{12h_x}\Big(\langle\phi\rangle_{i+1} - \langle\phi\rangle_{i-1}\Big) \\ &+ \frac{1}{12h_x}\Big(\langle\phi\rangle_{i+2} - \langle\phi\rangle_{i-2}\Big). \end{aligned} \tag{12}$$

To advance the solution $\langle f\rangle_{i,j}$ in time, it is necessary to calculate the distribution function flux entering each cell face of cell i, j. Based on the velocity and the electric field, the fourth-order accurate fluxes are calculated as follows:

$$\begin{aligned} \langle fv\rangle_{i+\frac{1}{2},j} = &\langle f\rangle_{i+\frac{1}{2},j}\langle v\rangle_{i+\frac{1}{2},j} \\ &+ \frac{h_v}{24}\Big(\langle f\rangle_{i+\frac{1}{2},j+1} - \langle f\rangle_{i+\frac{1}{2},j-1}\Big) \end{aligned} \tag{13}$$

$$\begin{aligned} \langle fE\rangle_{i,j+\frac{1}{2}} = &\langle f\rangle_{i,j+\frac{1}{2}}\langle E\rangle_{i,j+\frac{1}{2}} \\ &+ \frac{1}{48}\Big(\langle f\rangle_{i+1,j+\frac{1}{2}} - \langle f\rangle_{i-1,j+\frac{1}{2}}\Big) \\ &\cdot\Big(E_{i+1,j+\frac{1}{2}} - E_{i-1,j+\frac{1}{2}}\Big) \end{aligned} \tag{14}$$

Once the values of flux at each cell face are known, the Vlasov equation is reduced to an ordinary differential equation:

$$\begin{aligned} \frac{d\langle f\rangle_{i,j}}{dt} = &-\frac{1}{h_x}\left[\langle fv\rangle_{i+\frac{1}{2},j} - \langle fv\rangle_{i-\frac{1}{2},j}\right] \\ &+ \frac{e}{m}\frac{1}{h_v}\left[\langle fE\rangle_{i,j+\frac{1}{2}} - \langle fE\rangle_{i,j-\frac{1}{2}}\right]. \end{aligned} \tag{15}$$

Eq. 15 is integrated in time using a fourth-order explicit Runge-Kutta algorithm to advance $\langle f\rangle_{i,j}$ by a time step. The updated cell-average distribution function is then used to compute the electric field, and thus to advance the solution. This amounts to a fourth-order accurate discretization in time and space, using centered differencing for the latter.

IV. Single-Grid Simulation Results

The single grid algorithm described in the previous section is benchmarked against analytic results from kinetic theory. A standard test case is to simulate weak Landau damping by initializing a Maxwellian distribution in velocity space with a small position-dependent perturbation:

$$f(x,v)|_{t=0} = \frac{1}{\sqrt{2\pi}}\exp\left(-\frac{v^2}{2}\right)(1 + a\cos(kx)), \tag{16}$$

with $k = 0.5$ and $a = 0.01$. In weak Landau damping, potential energy (see Eq. 5) is transformed into thermal energy as indicated by a steady net decrease in the value of the former. The simulated decay rate of potential energy in time is in good agreement with the theoretical prediction, as shown in Fig. 1(a).

To test a non-linear regime of plasma kinetics, the simulation is benchmarked against theoretical predictions for strong Landau damping. In strong Landau damping, the Maxwellian

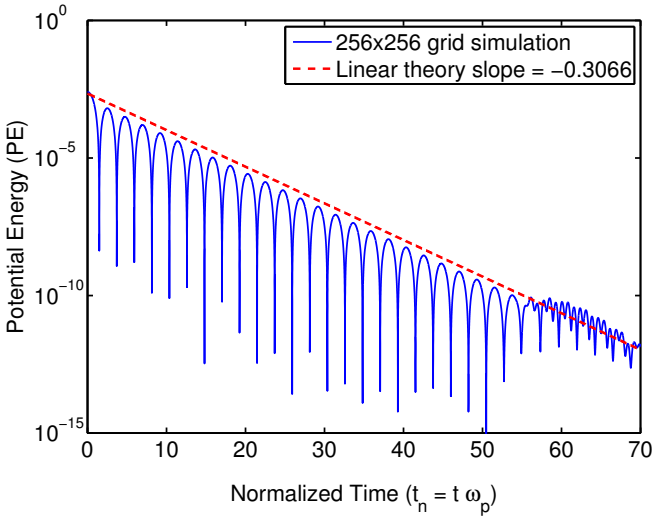

(a) Weak Landau damping

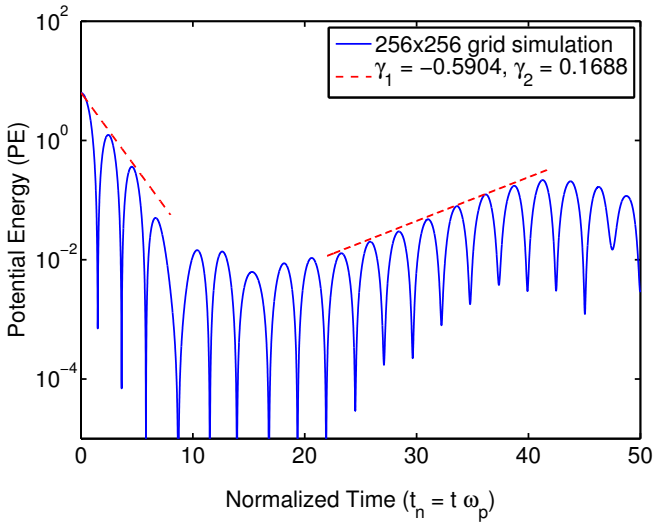

(b) Strong Landau damping

Fig. 1: Simulation results for (a) weak Landau damping and (b) strong Landau damping using a 256×256 grid. The evolution of potential energy demonstrates close agreement with theoretical predictions.

in Eq. 16 is given a large perturbation with amplitude $a = 0.5$. In this case, the potential energy in the system evolves non-linearly. This evolution is shown in Fig. 1(b), where the decay and growth rates in potential energy from the simulation are shown in comparison with theoretical predictions.

The algorithm is also used to simulate the two-stream instability. This simulation is initialized using the following distribution function

$$f(x,v)|_{t=0} = \frac{1}{\sqrt{2\pi}} v^2 \exp\left(-\frac{v^2}{2}\right)(1 + a\cos(kx)) \qquad (17)$$

with $k = 0.5$ and $a = 0.01$. The spatial perturbation results in inhomogeneities in the electron distribution such that kinetic energy is converted into potential energy. Fig. 2 shows how

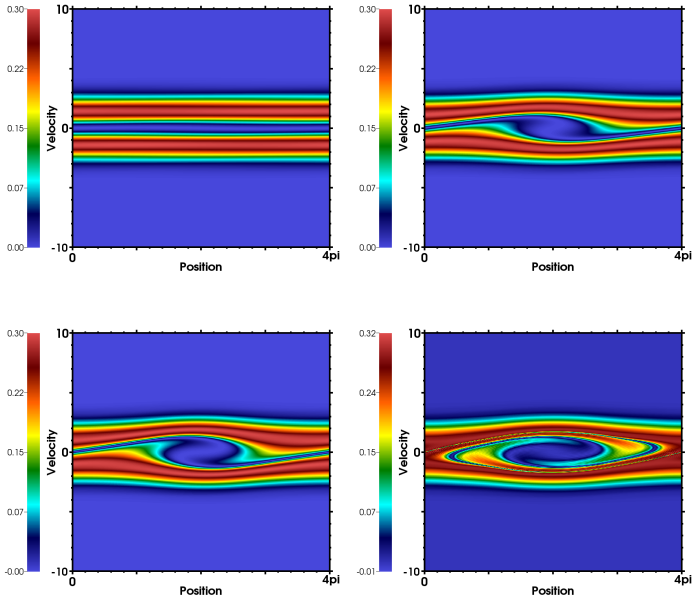

Fig. 2: Evolution of the two-stream instability for normalized time $t_n = 0, 18.8, 20.4, 29.8$. Note that at approximately $t = 18.8$ the instability becomes non-linear.

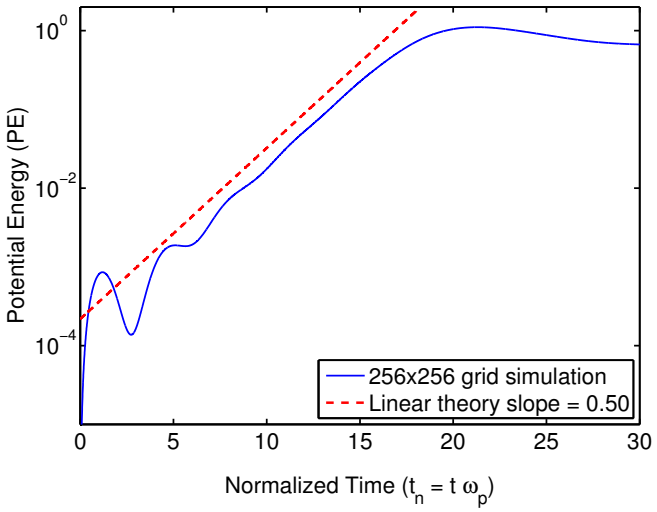

Fig. 3: The two-stream instability results demonstrate close agreement with theoretical predictions for the instability growth rate.

the electrons become trapped, as is evidenced by the formation of a vortex-like structure in the phase space distribution. It is important to note that dispersive effects, which can be seen at time $t = 29.8$, cause the distribution function to become negative in certain parts of the domain. This is an unphysical result that can be resolved through the use of limiters. When compared to linear theory, the growth rate in the potential energy resulting from the simulation is consistent with the theoretically predicted value for the two-stream instability, as shown in Fig. 3.

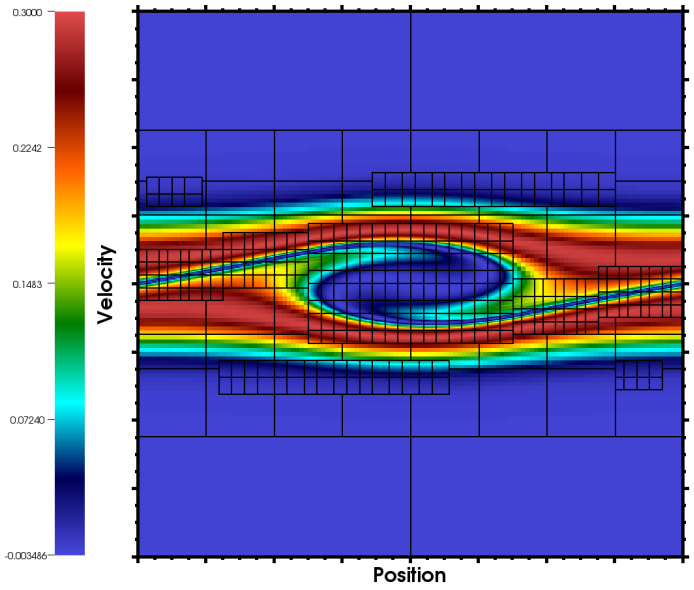

Fig. 4: Two-stream instability at $t = 22.1$. AMR simulation with 64×64 base grid, three levels of grid refinement, and a refinement ratio of four. Thus the smallest boxes indicate regions of the domain that have sixteen times the resolution of the coarsest grid.

.

V. Two-stream Instability with AMR

Adaptive mesh refinement is implemented into the single-grid algorithm described above, using the techniques described in Ref. [6]. As indicated in Eq. 3, the charge density is computed by taking a velocity moment of the distribution function at each spatial location. To do this on multiple levels of grids requires that additional interpolation steps be added to the AMR algorithm.

First a coarse-grid number density is computed using the coarse cell-average distribution function. The coarse grid number density is interpolated to the fine grid. In order to get the most accurate value of number density, the integral contribution from fine grid must be included. This is done by taking the difference between the coarse and fine distribution functions in regions where the fine grid exists, and integrating this difference with respect to v. This position-dependent contribution is then added to the interpolated coarse grid number density in spatial regions where the fine grid exists.

As a demonstration of adaptive mesh refinement capability, the two-stream instability is simulated using a three-level adaptively refined grid. The distribution function and grid are shown at time $t = 22.1$ in Fig. 4. The simulation uses a base grid of size 64×64 with a factor of four refinement for each successive level. Further analysis is required to evaluate the merits of AMR and to determine to what extent it reduces the computational cost of Vlasov-Poisson simulations.

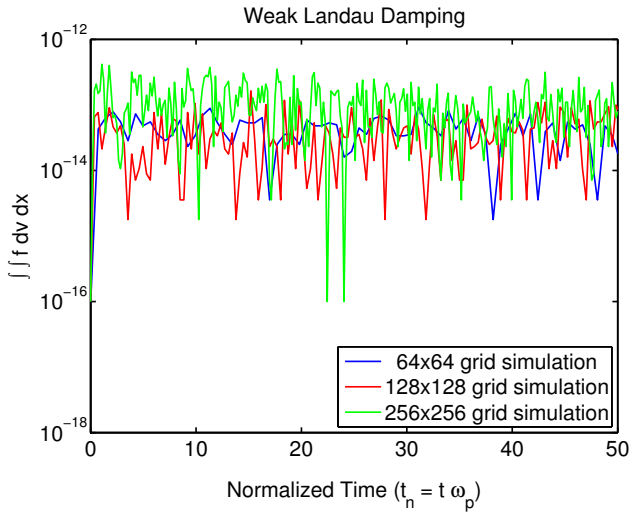

(a) Mass, zeroth moment

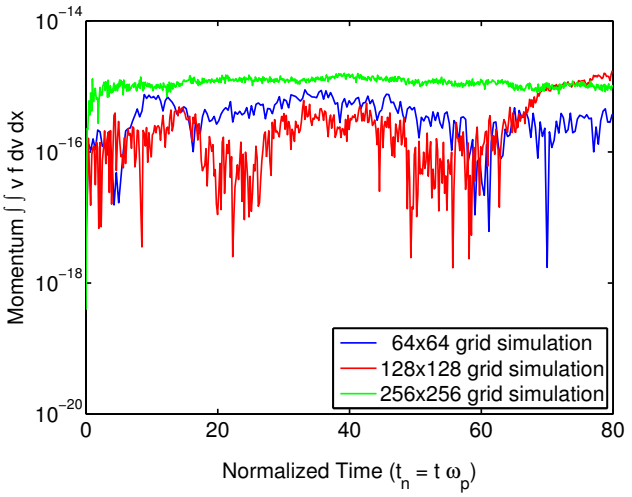

(b) Momentum, first moment

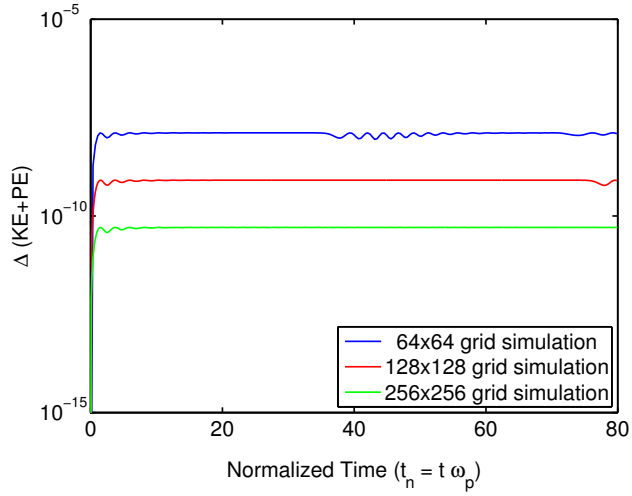

(c) Energy change relative to total energy at $t = 0$

Fig. 5: Absolute values of mass, momentum and energy for weak Landau damping. Mass is conserved to 10^{-13} precision, momentum is conserved to machine precision, and total energy conservation depends on the grid resolution.

VI. Conservation Properties

The conservation properties of the described algorithm are investigated by tracking the value of the zeroth, first, and second velocity moment of the distribution function (integrated over the entire domain) as a function of time. These integrals amount to conservation of mass, momentum and energy. Theoretically the value of each should be conserved to machine precision, but in practice numerical errors are introduced through the fourth-order approximation to the partial differential equation. Fig. 5 shows to what extent the mass, momentum, and energy of the system are conserved for the case of weak Landau damping. The zeroth moment is preserved to 10^{-13} independent of the grid resolution. The first moment is zero to machine precision, and its value is also independent of grid resolution. The second moment, as measured by the change in total energy relative to the initial value at $t = 0$, attains a value that is several orders of magnitude greater than machine precision. The second moment remains bounded for all time, and fourth-order convergence of the numerical method is demonstrated by the fact that the change in total energy decreases by a factor of approximately sixteen as the grid resolution is doubled in x and v. Conservation properties for non-linear plasma phenomena require further investigation.

VII. Conclusions

A fourth order accurate algorithm in space and time has been developed to solve the Vlasov-Poisson system in one spatial and one velocity dimension. The simulation results demonstrate close agreement with theoretical predictions, as tested on weak Landau damping, strong Landau damping, and the two-stream instability. AMR is also demonstrated as a practical means of reducing computational cost by focusing computational resources in dynamic regions of the domain. Further work needs to be done to assess the speed-up offered by adaptive mesh refinement, specifically as it applies in multiple dimensions. The described algorithm will also benefit from the use of limiters, which will address dispersive oscillations and lack of positivity preservation that are inherent to high-order finite volume calculations.

Acknowledgment

This research was supported in part by an award from the Department of Energy (DOE) Office of Science Graduate Fellowship Program (DOE SCGF). The DOE SCGF Program was made possible in part by the American Recovery and Reinvestment Act of 2009. The DOE SCGF program is administered by the Oak Ridge Institute for Science and Education for the DOE. ORISE is managed by Oak Ridge Associated Universities (ORAU) under DOE contract number DE-AC05-06OR23100. All opinions expressed in this paper are the author's and do not necessarily reflect the policies and views of DOE, ORAU, or ORISE.

References

[1] T. D. Arber and R. G. L. Vann. "A critical comparison of Eulerian-grid-based Vlasov solvers," *Journal of Computational Physics*, Vol. 180, No. 1, pp. 339-357, June 2002.

[2] J. W. Banks, and J. A. F. Hittinger. "A new class of nonlinear finite-volume methods for Vlasov simulation," *IEEE Transactions on Plasma Science*, Vol. 38, No. 9, September 2010.

[3] N. V. Elkina and J. Buchner. "A new conservative unsplit method for the solution of the Vlasov equation," *Journal of Computational Physics*, Vol. 213, No. 2, pp 862-875, April 2006.

[4] F. Filbet, E. Sonnendrucker. "Comparison of Eulerian Vlasov solvers," *Computer Physics Communications*, Vol. 150, No. 3, pp. 247-266, June 2002.

[5] R. T. Glassey. *Cauchy Problem in Kinetic Theory*, Society of Industrial and Applied Mathematics, Philadelphia, 1996.

[6] P. McCorquodale and P. Colella. "A High-Order Finite-Volume Method for Conservation Laws on Locally Refined Grids," *Communications in Applied Mathematics and Computational Science*, Vol. 6, No. 1, pp. 1-25, 2011

[7] N. J. Sircombe and T. D. Arber. "VALIS: A split-conservative scheme for the relativistic 2D Vlasov-Maxwell system," *Journal of Computational Physics*, Vol. 228, No. 13, pp 4773-4788, July 2009

[8] N. A. Krall and A. W. Trivelpiece. *Principles of plasma physics*, McGraw-Hill, 1973.

[9] B. Wang, G. H. Miller, and P. Colella. "A Particle-in-cell method with adaptive phase-space remapping for kinetic plasmas," *SIAM Journal of Scientific Computing, Vol. 33, No. 6, pp. 3509-3537*, September 2011.

[10] Q. Zhang, H. Johansen, and P. Colella. "A fourth-order accurate finite-volume method with structured adaptive mesh refinement for solving the advection-diffusion equation." *SIAM Journal of Scientific Computing*, Vol. 34, No. 2, pp. B179-B201, 2012